PERGAMON

Polyhedron 20 (2001) 1785–1793

POLYHEDRON

www.elsevier.com/locate/poly

Preparation, crystal structure and chelate substitution reactions of $[Mn_4O_2(O_2CPh)_6(dpm)_2]$ (dpm = the anion of dipivaloylmethane)

Cristina Cañada-Vilalta, John C. Huffman, George Christou *

Department of Chemistry and the Molecular Structure Center, Indiana University, Bloomington, IN 47405-7102, USA

Received 18 August 2000; accepted 3 October 2000

Abstract

The reaction of $[N^nBu_4][Mn_4O_2(O_2CPh)_9(H_2O)]$ with 2 equiv. of Na(dpm) (dpm^- is the anion of dipivaloylmethane) gives $[N^nBu_4][Mn_4O_2(O_2CPh)_7(dpm)_2]$ (**1**), which undergoes chelate substitution with picolinic acid (picH) or dibenzoylmethane (dbmH) to give the corresponding pic^- and dbm^- complexes, **2** and **3**, respectively. Reaction of **1** with 1 equiv. of Me_3SiCl converts it to $[Mn_4O_2(O_2CPh)_6(dpm)_2]$ (**4**), whose crystal structure shows a butterfly-like $[Mn_4O_2]^{8+}$ core but with two five-coordinate Mn^{III} ions. Compound **4** also undergoes chelate substitution with picH, dbmH, 2-(hydroxymethyl)pyridine and hexafluoroacetylacetone to give the corresponding complexes. With *trans*-1,2-*bis*(4-pyridyl)ethylene (bpe), a bridged compound $[Mn_4O_2(O_2CPh)_6(dpm)_2(bpe)]_2$ is obtained, analogous to the dbm^- compound previously characterized crystallographically. Magnetic susceptibility studies of **4** in the 5.00–300 K range give $J_{bb} = -27.5\ cm^{-1}$, $J_{wb} = -0.4\ cm^{-1}$ ($\hat{H} = -2J\hat{S}_i\hat{S}_j$ convention), and $g = 1.87$, indicating **4** to have a quintuply degenerate (n, 0, n) ground state ($n = 4$, 3, 2, 1, 0) as a result of the large J_{bb}/J_{wb} ratio. © 2001 Elsevier Science Ltd. All rights reserved.

Keywords: Crystal structures; Chelate substitution; Dipivaloylmethane; Picolinic acid; Tetranuclear Mn cluster; Magnetic susceptibility

1. Introduction

A variety of manganese carboxylate complexes have been prepared over the last several years in these laboratories as a result of our development of a number of new synthesis methodologies [1–7]. These efforts have been stimulated by a number of reasons, but the two main ones are: (i) the search for tetranuclear Mn complexes that are models of the similarly tetranuclear water oxidation complex (WOC) responsible for O_2 formation in the photosynthetic apparatus of green plants and cyanobacteria [8–10]; and (ii) the propensity of Mn clusters to possess ground state spin values that are often large and occasionally abnormally large [3,5] The latter property, when coupled to significant magnetoanisotropy as reflected in large values of the zero-field splitting parameter D, has led to the identification of the new magnetic phenomenon of single-molecule magnetism [11,12].

One synthetic method that has proved particularly useful to access new clusters is the reaction of Mn carboxylate species with a chelating ligand. The anion of dibenzoylmethane (dbmH) has proven especially useful, yielding, for example, complexes such as

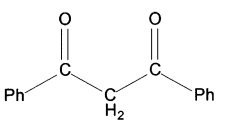

dbmH

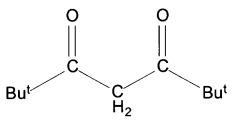

dpmH

$[Mn_4O_2(O_2CMe)_6(py)_2(dbm)_2]$ [13] and $(N^nBu_4)[Mn_4O_2(O_2CPh)_7(dbm)_2]$ [14] containing the $[Mn_4O_2]^{8+}$ core, which themselves have proven excellent stepping stones to the $[Mn_4O_3X]^{6+}$-containing complexes of formula $[Mn_4O_3X(O_2CR)_3(dbm)_3]$ ($X = PhCO_2^-$, $MeCO_2^-$, Cl^-, Br^-, F^-, N_3^-, NCO^-, etc.) [4,13,15,16]. Given the level of past success with dbm^-, we have explored the use of another β-diketonate in Mn carboxylate reactions, namely dipivaloylmethane (dpmH). This differs significantly from dbmH in its steric and electronic properties, which might be reflected in either the nature or reactivity of obtained products. In this report,

* Corresponding author. Tel./fax: +1-812-8552399.
E-mail address: christou@indiana.edu (G. Christou).

PII: S0277-5387(01)00761-6

we describe the methodology developed for the introduction of dpm^- into Mn_4 complexes, together with the resulting reactivity properties.

2. Experimental

2.1. Materials and methods

All manipulations were performed under aerobic conditions using chemicals as received unless otherwise stated. $Mn(O_2CPh)_2{\cdot}2H_2O$ [17], $(N^nBu_4)MnO_4$ [17] and $(N^nBu_4)[Mn_4O_2(O_2CPh)_9(H_2O)]$ [14] were prepared as described elsewhere.

2.2. Syntheses

Na(dpm)·3/4H$_2$O. A solution of $NaOCH_3$ (1.35 g, 25.0 mmol) in CH_3OH (125 ml) was treated with dpmH (5.20 ml, 25.0 mmol). The solution was stirred for 1 h and the solvent was removed to give the white salt, which was dried in vacuo. Yield: 84%. *Anal*. Found: C, 60.25; H, 9.44. Calc.: C, 60.12; H, 9.40%.

(N^nBu_4)[Mn$_4$O$_2$(O$_2$CPh)$_7$(dpm)$_2$]·2toluene (**1**). Solid Na(dpm)·3/4 H_2O (0.550 g, 2.50 mmol) was added to a stirred suspension of $(N^nBu_4)[Mn_4O_2(O_2CPh)_9(H_2O)]$ (2.00 g, 1.25 mmol) in toluene (100 ml). After 12 h, the mixture was filtered to remove a precipitate containing mainly $Na(O_2CPh)$. The filtrate was treated with hexanes (150 ml) and the subsequent dark brown precipitate was collected by filtration and redissolved in toluene (25 ml). The product was precipitated again with hexanes (50 ml), filtered, washed well with hexanes and dried in vacuo. Yield: 57%. *Anal*. Found: C, 61.42; H, 5.99; N, 0.99. Calc.: C, 61.46; H, 5.99; N, 0.82%.

(N^nBu_4)[Mn$_4$O$_2$(O$_2$CPh)$_7$(pic)$_2$] (**2**). To a brown solution of **1** (200 mg, 0.12 mmol) in MeCN (25 ml) was added solid picolinic acid (30 mg, 0.24 mmol). The mixture was stirred for 4 h during which time a dark precipitate formed. The latter was removed by filtration and the reddish brown filtrate was treated with a 1:1 (v/v) mixture of Et_2O and hexanes (25 ml), producing a precipitate that was collected by filtration, washed with Et_2O and dried in air. Yield: 29%. *Anal*. Found: C, 55.65; H, 3.87; N, 3.22. Calc.: C, 55.07; H, 3.91; N, 2.96%.

(N^nBu_4)[Mn$_4$O$_2$(O$_2$CPh)$_7$(dbm)$_2$]·0.25CH$_2$Cl$_2$ (**3**). To a brown solution of **1** (200 mg, 0.12 mmol) in CH_2Cl_2 (10 ml) was added solid dbmH (53 mg, 0.24 mmol). The mixture was stirred for 12 h with no appreciable change in color, filtered to remove a small amount of dark precipitate, and the filtrate treated with hexanes (20 ml) to give a precipitate that was collected by filtration, washed with Et_2O and dried in air. Yield: 70%. *Anal*. Found: C, 60.98; H, 4.37; N, 0.91. Calc.: C, 60.92; H, 4.27; N, 0.85%.

[Mn$_4$O$_2$(O$_2$CPh)$_6$(dpm)$_2$] (**4**). In Method A to a stirred dark brown solution of **1** (1.0 g, 0.59 mmol) in distilled MeCN (15 ml) was added Me_3SiCl (75 μl, 0.59 mmol) dropwise. The solution was stirred for a few minutes and then allowed to stand undisturbed overnight at room temperature (r.t.). The resulting black crystals were filtered, washed with MeCN and dried in air. Yield: 29%. *Anal*. Found: C, 56.31; H, 4.91; N, 0.61. Calc. for **4**·0.5MeCN: C, 56.23; H, 5.05; N, 0.50%.

In Method B a stirred solution of **1** (0.30 g, 0.18 mmol) in MeCN (15 ml) was treated with a 0.25M solution of triflic acid in MeCN (0.95 ml, 0.24 mmol). The solution was stirred for a few minutes and then left undisturbed for 1 h at r.t. Small black crystals were obtained, which were collected by filtration, washed with MeCN and dried in air. Yield: 41%. The identity of the product was confirmed by ^1H NMR and IR spectral comparison with the previous sample.

In Method C a mixture of $Mn(O_2CPh)_2{\cdot}2H_2O$ (0.40 g, 1.2 mmol) and benzoic acid (0.34 g, 2.8 mmol) in MeCN (25 ml) was stirred until complete dissolution. $(N^nBu_4)MnO_4$ (0.11 g, 0.30 mmol) dissolved in MeCN (4 ml) was added dropwise to the previous solution, which turned dark brown. Solid Na(dpm)·3/4H_2O (0.17 g, 0.75 mmol) was added to the mixture, and the system was stirred for 1 h, filtered to remove a black byproduct, and the filtrate left undisturbed for several hours. The resulting black crystals were collected by filtration, washed with MeCN and dried in air. Yield: 48% based on total Mn available. The product was identified as **4** by ^1H NMR and IR spectroscopies.

[Mn$_4$O$_2$(O$_2$CPh)$_6$(pic)$_2$]·0.25CH$_2$Cl$_2$ (**5**). Solid picolinic acid (35 mg, 0.29 mmol) was added to a stirred brown solution of **4** (200 mg, 0.14 mmol) in CH_2Cl_2 (15 ml). After 12 h the solution was treated with hexanes (3 ml) and left undisturbed for several hours at 5°C. The resulting reddish brown precipitate was separated by filtration and dried in vacuo. Yield: 8%. *Anal*. Found: C, 52.60; H, 3.16; N, 2.83. Calc.: C, 52.39; H, 3.12; N, 2.25%.

[Mn$_4$O$_2$(O$_2$CPh)$_6$(dbm)$_2$] (**6**). A brown solution of **4** (200 mg, 0.14 mmol) in CH_2Cl_2 (15 ml) was treated with dbmH (67 mg, 0.30 mmol) and the solution was stirred for 12 h without perceptible change in color. A precipitate was formed upon addition of hexanes (10 ml), which was collected by filtration, washed with Et_2O and dried in air. Yield: 12%. *Anal*. Found: C, 60.32; H, 4.13; N, 0.27. Calc.: C, 60.70; H, 3.68; N, 0.00%.

[Mn$_4$O$_2$(O$_2$CPh)$_6$(hmp)$_2$]·1/2H$_2$O (**7**). A small excess of hmpH (30 mg, 0.28 mmol) in CH_2Cl_2 (3 ml) was added to a stirred solution of $[Mn_4O_2(O_2CPh)_6(dpm)_2]$ (150 mg, 0.11 mmol) in CH_2Cl_2 (15 ml). The solution was stirred overnight and hexanes (5 ml) were added to precipitate a red–brown solid. This was collected by filtration, washed with hexanes and dried in air. Yield:

35%. *Anal*. Found: C, 53.49; H, 3.17. Calc.: C, 53.89; H, 3.60%.

$[Mn_4O_2(O_2CPh)_6(hfac)_2]\cdot 0.5CH_2Cl_2$ ***(8)***. To a brown solution of **4** (200 mg, 0.14 mmol) in CH_2Cl_2 (15 ml) was added excess hfacH (65μl, 0.46 mmol). The mixture was stirred for 3 h, concentrated under vacuum to half its volume, and treated with hexanes (10 ml). A brown precipitate formed and this was collected by filtration, redissolved in CH_2Cl_2 (8 ml) and treated again with hfacH (20 μl, 0.14 mmol). After stirring for several hours, the solution was concentrated and hexanes were added (5 ml). The resulting precipitate was collected by filtration and dried in air. Yield: 10%. *Anal*. Found: C, 44.03; H, 3.17; N, 0.18. Calc.: C, 43.95; H, 2.32; N, 0.00%.

$Na[Mn_4O_2(O_2CCH_3)_7(dpm)_2]\cdot 3H_2O$ ***(9)***. $Mn(O_2CCH_3)_2\cdot 4H_2O$ (3.92 g, 16.0 mmol) and $(N^nBu_4)Br$ (6.43 g, 20.0 mmol) were dissolved in a solvent mixture comprising MeCN (140 ml) and AcOH (6 ml). The resulting solution was stirred while solid $(N^nBu_4)MnO_4$ (1.45 g, 4.00 mmol) was added in small portions to give a very dark brown solution. Solid $Na(dpm)\cdot 3/4H_2O$ (2.19 g, 10 mmol) was then added, and the mixture was stirred for 3 h, filtered to separate a dark precipitate, and the filtrate concentrated to 75% of its initial volume. The solution was allowed to stand undisturbed overnight, resulting in the formation of green–brown crystals, which were collected by filtration, washed with Et_2O and dried in air and in vacuo. Yield: 36% based on total available Mn. *Anal*. Found: C, 38.72; H, 5.03; N, 0.08. Calc.: C, 39.01; H, 5.91; N, 0.00%.

$Na[Mn_4O_2(O_2CCH_3)_7(pic)_2]\cdot 3H_2O$ ***(10)***. Solid picolinic acid (44 mg, 0.36 mmol) was added to a slurry of **8** (200 mg, 0.18 mmol) in MeCN (15 ml) and the mixture was stirred overnight. An orange–brown precipitate was obtained, which was collected by filtration, washed with a little MeCN, and dried in air and in vacuo. Yield: 59%. *Anal*. Found: C, 31.72; H, 2.90; N, 2.80. Calc.: C, 32.42; H, 3.66; N, 2.91%.

$Na[Mn_4O_2(O_2CCH_3)_7(dbm)_2]\cdot 1.75CH_2Cl_2$ ***(11)***. A brown solution of **8** (200 mg, 0.18 mmol) in CH_2Cl_2 (14 ml) was treated with solid dbmH (81 mg, 0.36 mmol) and stirred overnight to give a green–brown precipitate that was collected by filtration, washed with Et_2O and dried in air and in vacuo. Yield: 57%. *Anal*. Found: C, 43.01; H, 3.62; N, 0.08. Calc.: C, 42.83; H, 3.65; N, 0.00%.

$[Mn_4O_2(O_2CPh)_6(dpm)_2(bpe)]_2$ ***(12)***. A solution of **4** (180 mg, 0.13 mmol) in CH_2Cl_2 (10 ml) was treated with solid bpe (25 mg, 0.13 mmol) and the mixture stirred for 20 min. Layering of the solution with Et_2O:hexanes (1:1) slowly produced dark, needle-shaped crystals, which were collected by filtration, washed with hexanes, and dried in air. Yield: 49%. *Anal*. Found: C, 59.47; H, 5.11; N, 1.77. Calc.: C, 59.82; H, 5.47; N, 1.79%.

Table 1
Crystallographic data for $[Mn_4O_2(O_2CPh)_6(dpm)_2]$ (**4**)[a]

Color	red–brown
Empirical formula	$C_{64}H_{68}O_{18}Mn_4$
Formula weight	1344.99
Crystal system	orthorhombic
Space group	$P2_12_12$
Unit cell dimensions	
a (Å)	16.419(3)
b (Å)	17.946(2)
c (Å)	10.682(1)
Temperature (°C)	−175
U (Å^3)	3147(2)
D_{calc} (g cm^{-3})	1.419
Z	2
Radiation, Mo Kα (Å)	0.71069 [a]
μ (cm^{-1})	8.540
Reflections collected	7040
Unique data	5546
R_{merge}	0.034
Reflections observed [b]	4163
$R(F)$ [c]	0.0415
$R_w(F)$ [d]	0.0348

[a] Graphite monochromator.
[b] $F > 2.33\sigma(F)$.
[c] $R = \Sigma \| |F_o| - |F_c| \| / \Sigma |F_o|$.
[d] $R_w = \left[\Sigma w(|F_o| - |F_c|)^2 / \Sigma w F_o^2 \right]^{1/2}$ where $w = 1/\sigma^2(|F_o|)$.

2.3. Crystal Structure of *4*

A red–brown, rectangular needle crystal was affixed to a glass fiber using silicone grease and transferred to the goniostat where it was cooled to −175°C for characterization and data collection. A systematic search of a limited hemisphere of reciprocal space determined that the crystal possessed orthorhombic symmetry and identified systematic absences corresponding to the space group $P2_12_12$. Subsequent successful solution and refinement of the structure confirmed this choice. The data were collected using standard procedures, and they were corrected for Lorentz and polarization effects, and equivalent reflections were averaged. The structure was solved using direct methods (MULTAN78) and standard Fourier techniques. The absolute structure was determined by examination of the residuals using the two possible structures. All non-hydrogen atoms were readily located without disorder problems and refined anisotropically. Hydrogen atoms were located in a difference Fourier map phased on the non-hydrogen atoms, and were refined isotropically in the final refinement cycles. A final difference Fourier map was essentially featureless, the largest peak being of intensity 0.55 e Å^{-3}. The crystal data and structure solution details are given in Table 1.

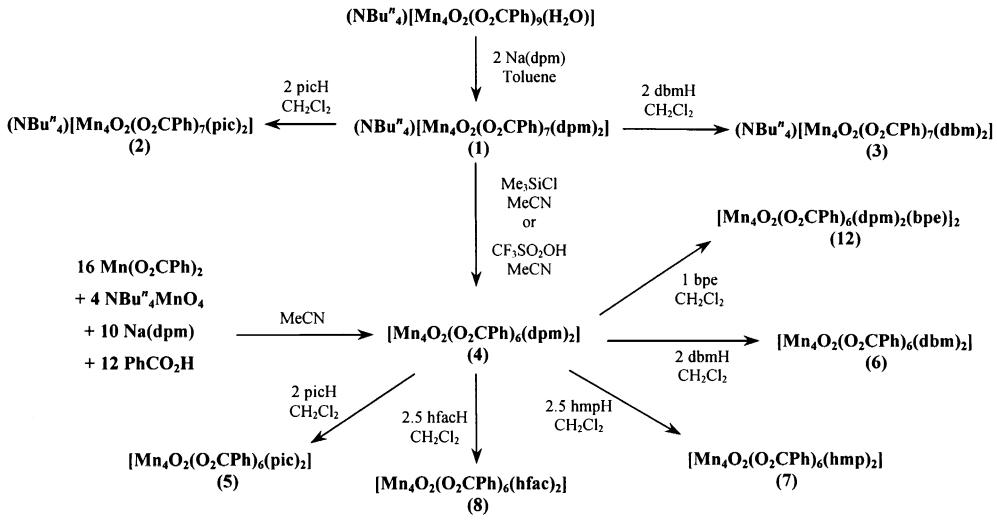

Scheme 1.

2.4. Other measurements

Electrochemical studies were performed in MeCN solution containing 0.1 M $N^nBu_4PF_6$ as supporting electrolyte, using a standard three-electrode assembly (glassy carbon working, Pt wire auxiliary, and SCE reference electrodes). Cyclic voltammetry (CV) and differential pulse voltammetry (DPV) were both employed, at scan rates of 100 and 20 mV s^{-1}, respectively. ^{1}H NMR spectra were obtained at 300 MHz on a Varian Gemini 2000 spectrometer. Magnetochemical studies were performed on microcrystalline samples restrained in eicosane to prevent torquing with a Quantum Design MPMS XL SQUID susceptometer using a 1 T DC field and a temperature range of 5.00–300 K.

3. Results and discussion

3.1. Syntheses

For convenience, the preparations and transformations described in this paper are summarized in Schemes 1 and 2.

We had previously shown that the reaction of $[Mn_4O_2(O_2CPh)_9(H_2O)]^-$, a $[Mn_4O_2]^{8+}$ butterfly complex but with only carboxylate and H_2O ligands, is a good route to picolinate (pic^-)- or dbm^--containing complexes [14], and the same route with Na(dpm) successfully gave the complex $(N^nBu_4)[Mn_4O_2(O_2CPh)_7(dpm)_2]$ **1** (Eq. (1)).

$$[Mn_4O_2(O_2CPh)_9(H_2O)]^- + 2dpm^- \rightarrow [Mn_4O_2(O_2CPh)_7(dpm)_2]^- + 2PhCO_2H + H_2O \quad (1)$$

Unlike dbmH (where the use of the protonated form gives a reaction to yield $[Mn_4O_2(O_2CPh)_7(dbm)_2]^-$), dpmH will not react with $[Mn_4O_2(O_2CPh)_9(H_2O)]^-$, presumably due to its lower acidity (pK_a 11.57) [18] compared with dbmH (8.95) [18], which inhibits the reaction. The high pK_a of dpmH is an advantage, however, in enabling chelate-substitution reactions to occur with picH (pK_a 5.39) [18] or dbmH. Stoichiometric addition of these chelates to **1** leads to formation of the substituted products **2** and **3** with no attack at carboxylate positions, fragmentation of the complex into dinuclear units, or other side-reactions being evident (Eq. (2); chelH = picH or dbmH).

$$[Mn_4O_2(O_2CPh)_7(dpm)_2]^- + 2chelH \rightarrow [Mn_4O_2(O_2CPh)_7(chel)_2]^- + 2dpmH \quad (2)$$

In previous work we had shown how one RCO_2^- group in $[Mn_4O_2(O_2CR)_7(pic)_2]^-$ is unique in having both its O atoms on Jahn–Teller (JT) elongation sites

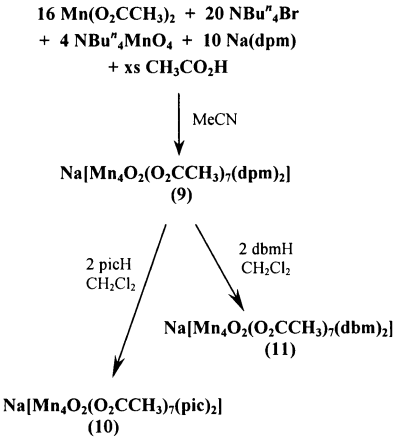

Scheme 2.

[19]. This makes this RCO_2^- group more susceptible to electrophilic attack and can be selectively abstracted by Me_3SiCl. Application of this methodology to **1** allows for its conversion to neutral $[Mn_4O_2(O_2CPh)_6(dpm)_2]$ **4** (Eq. (3)). Triflic acid also converts **1** to **4**, but further equivalents of Me_3SiCl or triflic acid cause decomposition of the complex.

$$[Mn_4O_2(O_2CPh)_7(dpm)_2]^- + Me_3SiCl \rightarrow [Mn_4O_2(O_2CPh)_6(dpm)_2] + Me_3SiO_2CPh \quad (3)$$

Complex **4** was subsequently obtained by a more direct method involving a comproportionation reaction between $Mn(O_2CPh)_2$ and MnO_4^- in the presence of Na(dpm) and $PhCO_2H$ (Eq. (4)) (Selected interatomic distances and angles of complex **4** are presented in Table 2). The identity of **4** was confirmed by crystallography, which also indicated two five-coordinate Mn^{III} ions at the central or body positions of the $[Mn_4O_2]^{8+}$ butterfly unit (see below).

$$16Mn^{II} + 4Mn^{VII} \rightarrow 5Mn_4^{III} \quad (4)$$

3.2. Reactivity characteristics of compound *4*

It has recently been established that treatment of $[Mn_4O_2(O_2CEt)_6(dbm)_2]$ with 1 to 2 equiv. of mineral acids HX (X = F, Cl, Br, NO_3) results in the formation via disproportionation of the $[Mn_4O_3X(O_2CEt)_3(dbm)_3]$ complexes [15]. This process is triggered by carboxylate abstraction and is analogous to the same transformation previously established using Me_3SiX (X = Cl, Br) [16]. Similar reactions with **4** do not, however, lead to $[Mn_4O_3X]^{6+}$ products. Precipitation of solids with the characteristic IR signatures of Mn oxides was observed, and free dpmH was identified by NMR examination of the filtrate. The difference in behavior between dbm^- and dpm^- complexes is again attributed to the greater basicity of the latter, and protonation and release of dpmH is likely the initiator of the decomposition.

Once again, however, the basicity of dpm^- can be employed for chelate substitution reactions as shown in Scheme 1. Thus, treatment of **4** with more acidic picH, dbmH and 2-(hydroxymethyl)pyridine (hmpH) allows formation of the corresponding $[Mn_4O_2(O_2CPh)_6(chel)_2]$ complexes **5**, **6** and **7** with release of dpmH. The advantage of this chelate-substitution reaction is emphasized by the preparation of a compound not accessible by other means: use of hexafluoroacetylacetone (hfacH) leads to $[Mn_4O_2(O_2CPh)_6(hfac)_2]$ (**8**). The highly electron-withdrawing CF_3 groups not only make hfacH very acidic (pK_a 4.35) [20] and thus appropriate for an acid-promoted substitution, but they also make the conjugate base $hfac^-$ a poor ligand. Thus, $hfac^-$ rarely forms stable compounds with transition metals in high oxidation states; the only previous well-characterized Mn^{III}–$hfac^-$ complex is $Mn(hfac)_3$ [21].

In order to obtain a dpm^- complex with acetate groups, the comproportionation method was employed and this successfully gave $Na[Mn_4O_2(O_2CMe)_7(dpm)_2]$ (**9**) from which could readily be obtained the corresponding pic^- and dbm^- complexes **10** and **11**, respectively, by chelate substitution, as shown in Scheme 2. We have previously demonstrated facile carboxylate substitution reactions in $[Mn_4O_2]^{8+}$ complexes by treatment of the acetate derivative with carboxylic acids more acidic than acetic acid [1,22]. Such reactions with **9**–**11** would likely lead to carboxylate derivatives of choice, but such transformations have not been explored in the present work.

All products were characterized by elemental analysis and spectroscopic (NMR, IR) comparisons with authentic materials from previous work, except for the dpm^- compounds and the other new compounds **7**, **8** and **11**.

3.3. Linkage of two $[Mn_4O_2]$ units

The uncommon structure of **4** containing a butterfly topology with two central pentacoordinated Mn^{III} ions possesses little steric impediment to the approach of a sixth ligand to each metal. Thus, the possibility of bridging two $[Mn_4O_2]$ units by *trans*-1,2-bis(4-pyridyl)ethylene (bpe) was investigated and established. Treatment of **4** with 1 equiv. of bpe leads to isolation of needle-like crystals whose elemental analysis, and IR and NMR characteristics indicate the formulation $[Mn_4O_2(O_2CPh)_6(dpm)_2(bpe)]_2$ (**12**) analogous to the crystallographically characterized dbm^- complex reported earlier containing two $[Mn_4O_2(O_2CPh)_6(dbm)_2]$ units bridged by two bpe groups [23].

Table 2
Selected interatomic distances (Å) and angles (°) for complex **4**

Interatomic distances			
Mn(1)–Mn(1′)	2.841(1)	Mn(1)–O(24)	2.071(3)
Mn(1)–Mn(2)	3.255(1)	Mn(2)–O(3)	1.890(3)
Mn(1)–Mn(2′)	3.362(1)	Mn(2)–O(6)	2.186(3)
Mn(2)–Mn(2′)	5.578(1)	Mn(2)–O(15)	2.169(3)
Mn(1)–O(3)	1.865(3)	Mn(2)–O(22)	1.959(3)
Mn(1)–O(3′)	1.883(3)	Mn(2)–O(31)	1.941(3)
Mn(1)–O(4′)	1.922(3)	Mn(2)–O(35)	1.903(3)
Mn(1)–O(13)	1.938(3)		
Interatomic angles			
O(3)–Mn(1)–O(3′)	81.46(13)	O(3)–Mn(2)–O(15)	91.89(12)
O(3′)–Mn(1)–O(4′)	92.17(13)	O(3)–Mn(2)–O(22)	94.43(13)
O(3)–Mn(1)–O(4′)	165.77(14)	O(3)–Mn(2)–O(31)	87.96(12)
O(3)–Mn(1)–O(13)	94.27(12)	O(3)–Mn(2)–O(35)	178.18(13)
O(3′)–Mn(1)–O(13)	159.21(13)	O(6)–Mn(2)–O(15)	170.87(12)
O(3)–Mn(1)–O(24)	95.09(13)	O(6)–Mn(2)–O(22)	98.84(12)
O(3′)–Mn(1)–O(24)	104.45(12)	O(6)–Mn(2)–O(31)	85.47(12)
O(4′)–Mn(1)–O(13)	87.19(13)	O(6)–Mn(2)–O(35)	90.42(12)
O(4′)–Mn(1)–O(24)	98.82(12)	O(15)–Mn(2)–O(22)	90.23(12)
O(13)–Mn(1)–O(24)	96.18(12)	O(15)–Mn(2)–O(31)	85.42(12)
O(3)–Mn(2)–O(6)	88.46(11)		

3.4. Description of the structure of $[Mn_4O_2(O_2CPh)_6(dpm)_2]$

This compound crystallizes in the space group $P2_12_12$. The unit cell contains two molecules of the neutral complex and there are four asymmetric units per cell, i.e. the asymmetric unit consists of half of the Mn_4 cluster. The structure (Fig. 1) can be described as a $[Mn_4(\mu_3\text{-}O)_2]$ butterfly core with two pentacoordinated Mn(1) atoms occupying 'body' sites and two hexacoordinated, distorted octahedral Mn(2) atoms in the wingtip sites. The only crystallographic symmetry element through the molecule is a C_2 axis perpendicular to the Mn(1)–O(3)–Mn(1′)–O(3′) plane. Each Mn(2) atom is bridged to the two central Mn(1) atoms through a μ_3-oxide: both oxide anions lie under the triangular planes formed by Mn(1)–Mn(1′)–Mn(2) and Mn(1)–Mn(1′)–Mn(2′), respectively. The dihedral angle between these two planes is 138°. Central and wingtip Mn atoms are also connected through two (between Mn(1) and Mn(2)) and one (between Mn(1)and Mn(2′)) benzoate bridges. The peripheral ligation is completed by two terminal, symmetry-equivalent, dpm^- chelate groups attached to the wingtip ions.

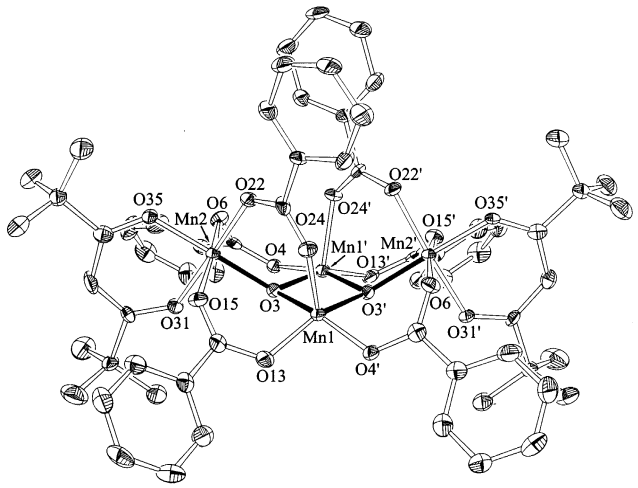

Fig. 1. ORTEP representation of $[Mn_4O_2(O_2CPh)_6(dpm)_2]$ (**4**) showing 50% probability ellipsoids.

Table 3
Electrochemical data [a] for the oxidation of $[Mn_4O_2(O_2CPh)_x(chel)_2]^z$ ($x = 6$ or 7) complexes

Complex	E_p (V)	pK_a [b]
$[Mn_4O_2(O_2CPh)_6(dpm)_2]$ (**4**)	0.91	11.57
$[Mn_4O_2(O_2CPh)_7(bpy)_2](ClO_4)$	0.90	
$(N^nBu_4)[Mn_4O_2(O_2CPh)_7(pic)_2]$ (**2**)	0.68	5.39
$(N^nBu_4)[Mn_4O_2(O_2CPh)_7(dbm)_2]$ (**3**)	0.42	8.95
$(N^nBu_4)[Mn_4O_2(O_2CPh)_7(hmp)_2]$	0.38	12.90
$(N^nBu_4)[Mn_4O_2(O_2CPh)_7(dpm)_2]$ (**1**)	0.29	11.57

[a] Quoted potentials are DPV peak potentials in MeCN vs ferrocene.

[b] Of the conjugate acid measured in H_2O (picH, dbmH, dpmH) [18] or H_2O/dioxan (1:1 v/v) (hmpH) [26].

All the metals are in the +3 oxidation state: the two central Mn(1) atoms are pentacoordinated and possess square-pyramidal geometry ($\tau = 0.109$, where $\tau = 0$ and 1 for sp and tbp geometries, respectively) [24], with O(24) being in the axial position. Thus, Mn(1)–O(24) is significantly longer (2.071(3) Å) than the other Mn(1)–O bonds (1.865(3)–1.938(3) Å). The two Mn atoms in the wingtip positions are hexacoordinated and, as expected for high spin Mn^{III} in near octahedral geometry, are Jahn–Teller distorted. Their geometry is that of an elongated octahedron, with the Jahn–Teller elongation axes passing through O(15)–Mn(2)–O(6), parallel to each other and almost perpendicular (88°) to the axes of the square-pyramids.

The butterfly-like $[Mn_4O_2]^{8+}$ core has been previously seen in several complexes, such as (N^nBu_4)-$[Mn_4O_2(O_2CMe)_7(pic)_2]$ [22] and $(N^nBu_4)[Mn_4O_2$-$(O_2CPh)_8(dbm)]$ [14]. However, very few previous examples of pentacoordinated Mn have been reported in Mn carboxylate chemistry, and complex **4** represents the first case of this coordination number in a butterfly rather than a planar Mn_4 topology. The closest previous example is $[Mn_4O_2(O_2CPh)_6(py)(dbm)_2]$ [25] where, however, only one of the body Mn^{III} ions is pentacoordinated, the other containing a py group and thus hexacoordinated.

3.5. Electrochemistry

The electrochemical properties of selected complexes were studied by CV and DPV in MeCN, and the results are collected in Table 3. Complexes **1** and **4** show the same quasi-reversible oxidation process previously observed for complexes with the other chelate ligands [1,22,27]. The potentials in Table 3 (the DPV peak positions) show a large difference between **1** (0.29 V) and **4** (0.91 V) reflecting the extra $PhCO_2^-$ group in the former and the resulting negative charge of the cluster that make the oxidation more facile. Comparing only complexes **1**–**3** and $(N^nBu_4)[Mn_4O_2(O_2CPh)_7(hmp)_2]$, which have the same formulation and charge, the oxidation potential approximately correlates with the basicity of the chelate group as reflected in the pK_a values of the conjugate acids, i.e. the oxidation potential decreases as the chelate becomes a better donor of electron density. The redox process occurring corresponds to the formation of the $3Mn^{III}$, Mn^{IV} complex, i.e. $[Mn_4O_2(O_2CPh)_7(chel)_2]$ but its quasi-reversible nature has been previously identified for **3** as due to subsequent reaction of the oxidized species with H_2O to give $[Mn_4O_3(O_2CPh)_4(dbm)_3]$ [4], isolated after controlled potential electrolysis studies. No doubt the other $[Mn_4O_2(O_2CPh)_7(chel)_2]^-$ complexes undergo related

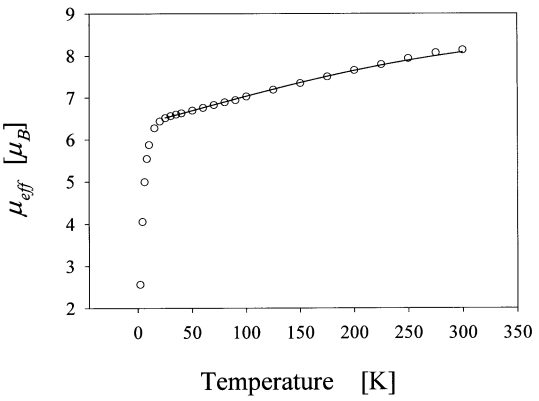

Fig. 2. Plot of effective magnetic moment (μ_{eff}/Mn_4) for $[Mn_4O_2(O_2CPh)_6(dpm)_2]$ (**4**). The solid line is a fit of the 25.0–300 K data to the theoretical equation; see the text for the fitting parameters.

reactions after oxidation, but this has not been explored in comparable detail yet. One final useful comparison in Table 3 can be made between **4** and $[Mn_4O_2(O_2CPh)_7(bpy)_2]^{+}$ (bpy = 2,2′-bipyridine). The former has a much higher oxidation potential than **1** because it has only six carboxylates and is neutral; the bpy complex has a similar potential to **4** even though it has seven carboxylates because the neutral bpy is a poorer base than dpm^{-} and also imparts a positive charge to the cluster, making electron abstraction more difficult.

3.6. Magnetochemistry

The magnetic susceptibility of **4** was measured in the 5.00–300 K temperature range. The effective magnetic moment (μ_{eff}) per Mn_4 gradually decreases from $8.23\mu_B$ at 300 K to $6.65\mu_B$ at 20.0 K and then decreases more rapidly to $4.90\mu_B$ at 5.00 K (Fig. 2). These correspond to $\chi_M T$ values of 8.47, 5.53 and 3.00 $cm^3\,K\,mol^{-1}$ at the three temperatures, respectively. The data were fit to the model previously employed for related $[Mn_4O_2]^{8+}$ butterfly complexes with a C_{2v} core symmetry [1,22]. This model involves two pairwise exchange interaction constants: J_{bb} for the body–body interaction (Mn(1)–Mn(1′) in Fig. 1) and J_{wb} for the wingtip–body interactions (Mn(1)–Mn(2), Mn(1) and Mn(2′) and the symmetry-related interactions). As previously, Mn_2 wingtip–body pairs bridged by one or two carboxylate groups are considered as equivalent since the superexchange mechanism is primarily through the O^{2-} bridges and thus essentially equivalent for the two possibilities. Under C_{2v} core symmetry, the appropriate spin Hamiltonian is that in Eq. (5). On applying the Kambe method [28],

$$\hat{H} = -2J_{bb}\hat{S}_1\hat{S}_{1'} + 2J_{wb}(\hat{S}_1\hat{S}_2 + \hat{S}_1\hat{S}_{2'} + \hat{S}_{1'}\hat{S}_2 + \hat{S}_{1'}\hat{S}_{2'}) \quad (5)$$

using the substitutions $\hat{S}_{bb} = \hat{S}_1 + \hat{S}_{1'}$, $\hat{S}_{ww} = \hat{S}_2 + \hat{S}_{2'}$ and $\hat{S}_T = \hat{S}_{bb} + \hat{S}_{ww}$, the spin Hamiltonian can be transformed to an equivalent one whose eigenvalues are given in Eq. (6), where constant terms have been ignored. For four Mn^{III} ions ($S = 2$) the total system consists of 85 possible spin states with S_T ranging from 0 to 8. Using Eq. (6) and the Van Vleck equation [29],

$$E = -J_{bb}[S_{bb}(S_{bb}+1)] - J_{wb}[S_T(S_T+1) - S_{bb}(S_{bb}+1) - S_{ww}(S_{ww}+1)] \quad (6)$$

a theoretical χ_M versus T equation was derived to fit the experimental data. The fit is shown as μ_{eff} versus T in Fig. 2. Only data above 25 K were employed to avoid those effects that show up at low temperature (primarily intermolecular interactions and zero-field splitting) that the theoretical model does not take into account, but which result in the rapid decrease in μ_{eff} below 25 K. The fitting parameters were $J_{bb} = -27.5(7)\ cm^{-1}$, $J_{wb} = -0.4(2)\ cm^{-1}$ and $g = 1.87$, with temperature-independent paramagnetism (TIP) held constant at $800 \times 10^{-6}\ cm^3\,mol^{-1}$. These parameters identify the ground state to be fivefold degenerate; in the format (S_T, S_{bb}, S_{ww}), the ground state is (n, 0, n) where $n = 4$, 3, 2, 1 and 0. The first excited state is (3, 1, 4) at 51 cm^{-1} above the ground state.

All previous magnetochemically characterized $[Mn_4O_2]^{8+}$ complexes (Table 4) have had a (3, 1, 4) ground state ($S_T = 3$), so the finding of a quintuply degenerate (n, 0, n) ground state was surprising. The reason lies in the relative magnitude of the two exchange parameters, i.e. the J_{bb}/J_{wb} ratio. The rhomboidal $[Mn_4O_2]$ unit has been identified previously as an example of a species exhibiting spin frustration [22], defined as the presence of competing exchange interactions of comparable magnitude such that the preferred spin alignments in the ground state are prevented (frustrated). The ground state then becomes highly sensitive to the relative magnitude (or ratio) of the competing exchange interactions. In the $[Mn_4O_2]^{8+}$ units all J values are negative (antiferromagnetic) but it is not possible to simultaneously align all the interacting spins in an antiparallel manner. Although $J_{bb} > J_{wb}$, there are more of the latter pairwise interactions than the former. For previously studied $[Mn_4O_2]^{8+}$ species, the J_{bb}/J_{wb} ratio is 3.0 to 5.0 and the (S_T, S_{bb}, S_{wb}) = (3, 1, 4) ground state can be depicted diagrammatically as shown:

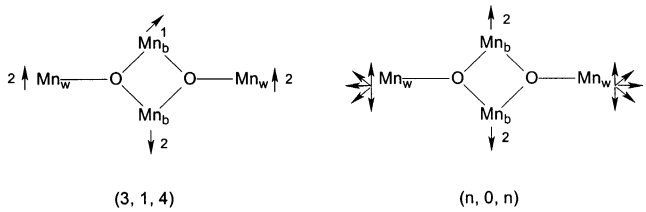

Table 4
Exchange parameters and ground state spin for selected $[Mn_4O_2]^{8+}$ complexes[a]

Compound	J_{wb} [a]	J_{bb} [a]	J_{bb}/J_{wb}	g	(S_T, S_{bb}, S_{ww})
$[Mn_4O_2(O_2CMe)_7(bpy)_2](ClO_4)$ [b]	−7.8	−23.5	3.0	2.00	(3, 1, 4)
$(N^nBu_4)[Mn_4O_2(O_2Cme)_7(pic)_2]$ [c]	−5.3	−24.6	4.6	1.96	(3, 1, 4)
$[Mn_4O_2(O_2CMe)_6(py)_2(dbm)_2]$ [d]	−5.0	−24.9	5.0	1.88	(3, 1, 4)
$[Mn_4O_2(O_2CPh)_6(dpm)_2]$ [e]	−0.4	−27.5	68.8	1.87	(n, 0, n)

[a] In cm^{-1}.
[b] Ref. [1].
[c] Ref. [22].
[d] Ref. [9].
[e] This work.

the two Mn_b ions are equivalent and coupled together, so this diagram is to be interpreted as showing that the two body spins give a resultant $S_{bb} = 1$ (rather than 0), which couples with the $S_{ww} = 4$ to give $S_T = 3$. In complex **4**, however, the J_{bb}/J_{wb} ratio is much larger (69) and the J_{wb} interactions cannot frustrate the antiparallel alignment of the Mn_b spins to give $S_{bb} = 0$. In effect, the ground state can be thought of as consisting of two Mn_w ions separated by a diamagnetic ($S_{bb} = 0$) $[Mn_{b2}O_2]$ unit: in the absence of any long-range interaction between the two Mn_w ions (i.e. $J_{ww} = 0$), all orientations of the individual Mn_w spins are equivalent and the ground state is fivefold degenerate. An alternative and completely equivalent description is to say the ground state is composed of two non-interacting independent Mn^{III} ions. It is tempting to assume that the decrease in μ_{eff} below 25 K is due only to the weak, long-range Mn_w–Mn_w interaction (J_{ww}), and thus include this in the Hamiltonian and include J_{ww} in a fit of the low-temperature data. However, single-ion zero-field splitting and intermolecular interactions (J_{inter}) would be of comparable magnitude to J_{ww}, and the assumption that the low-temperature behavior is due only to J_{ww} is invalid.

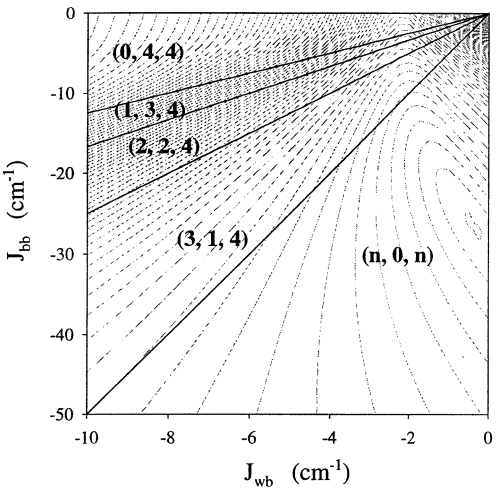

Fig. 3. Two-dimensional contour plot of the error surface for the fit of the data for **4**. Dashed lines represent the relative error, while solid lines define the boundaries between areas of different values of (S_T, S_{bb}, S_{ww}).

Fig. 3 conveniently depicts in one plot two important points: (i) the ground state (S_T, S_{bb}, S_{ww}) is shown for various regions of the J_{bb} versus J_{wb} space, clearly indicating that the boundary between the (3, 1, 4) and (n, 0, n) regions occurs at $J_{bb}/J_{wb} \approx 5$; and (ii) the minimum in the root-mean-square error surface for the fitting lies well within the (n, 0, n) region so that fitting uncertainties in the precise values of J_{bb} and J_{wb} (and hence the J_{bb}/J_{wb} ratio) do not affect the conclusion that **4** has a (n, 0, n) ground state.

4. Conclusions

The dpm^- chelate can successfully be incorporated into a tetranuclear Mn carboxylate complex. Its high basicity is an advantage in providing a ready means for the first time of chelate substitution in $[Mn_4O_2]$ complexes with chelates whose conjugate acids are more acidic than dpmH. However, the high basicity of dpm^- is also a disadvantage in other reactions, compared with dbm^-; while compounds with the latter can be cleanly oxidized to Mn^{IV}-containing products, the dpm^- species cannot. The unusual structure of **4** and its resulting (n, 0, n) ground state provides a new and useful datum point in the continuing search for an understanding of the factors that control the ground state in clusters containing competing exchange interactions and spin frustration effects.

5. Supplementary material

Crystallographic data for the structural analysis has been deposited with the Cambridge Crystallographic Data Center, CCDC No. 148270. Copies of this information may be obtained free of charge from The Director, CCDC, 12 Union Road, Cambridge CB2 1EZ, UK (fax: +44-1223-336033; e-mail: deposit@ccdc.cam.ac.uk or www: http://www.ccdc.cam.ac.uk).

Acknowledgements

This work was supported by the National Institute of Health.

References

[1] J.B. Vincent, C. Christmas, H.-R. Chiang, Q. Li, P.D.W. Boyd, J.C. Huffman, D.N. Hendrickson, G. Christou, J. Am. Chem. Soc. 111 (1989) 2086.
[2] S. Wang, H.-L. Tsai, W.E. Streib, G. Christou, D.N. Hendrickson, J. Chem. Soc., Chem. Commun. (1992) 1427.
[3] G. Aromí, M.J. Knapp, J.-P. Claude, J.C. Huffman, D.N. Hendrickson, G. Christou, J. Am. Chem. Soc. 121 (1999) 5489.
[4] S. Wang, H.-L. Tsai, K.S. Hagen, D.N. Hendrickson, G. Christou, J. Am. Chem. Soc. 116 (1994) 8376.
[5] A.R. Schake, H.-L. Tsai, N. de Vries, R.J. Webb, K. Folting, D.N. Hendrickson, G. Christou, J. Chem. Soc., Chem. Commun. (1992) 181.
[6] H.J. Eppley, S.M.J. Aubin, W.E. Streib, J.C. Bollinger, D.N. Hendrickson, G. Christou, Inorg. Chem. 36 (1997) 109.
[7] G. Aromí, S.M.J. Aubin, M.A. Bolcar, G. Christou, H.J. Eppley, K. Folting, D.N. Hendrickson, J.C. Huffman, R.C. Squire, H.-L. Tsai, S. Wang, M.W. Wemple, Polyhedron 17 (1998) 3005.
[8] N.A. Law, M.T. Caudle, V.L. Pecoraro, in: A.G. Sykes (Ed.), Advances in Inorganic Chemistry, vol. 46, Academic Press, London, 1998, p. 305.
[9] V.L. Pecoraro, A. Gelasco, M.J. Baldwin, Adv. Chem. Ser. 246 (1993) 205.
[10] P.J. Riggs-Gelasco, R. Mei, J.E. Penner-Hahn, Adv. Chem. Ser. 246 (1993) 219.
[11] H.J. Eppley, H.-L. Tsai, N. de Vries, K. Folting, G. Christou, D.N. Hendrickson, J. Am. Chem. Soc. 117 (1995) 301.
[12] S.M.J. Aubin, M.W. Wemple, D.M. Adams, H.-L. Tsai, G. Christou, D.N. Hendrickson, J. Am. Chem. Soc. 118 (1996) 7746.
[13] S. Wang, K. Folting, W.E. Streib, E.A. Schmitt, J.K. McCusker, D.N. Hendrickson, G. Christou, Angew. Chem. 103 (1991) 314; Angew. Chem. Int. Ed. Engl. 30 (1991) 305.
[14] M.W. Wemple, H.-L. Tsai, S. Wang, J.-P. Claude, W.E. Streib, J.C. Huffman, D.N. Hendrickson, G. Christou, Inorg. Chem. 35 (1996) 6437.
[15] G. Aromí, S. Bhaduri, P. Artús, K. Folting, J.C. Huffman, G. Christou, submitted for publication.
[16] S. Wang, H.-L. Tsai, E. Libby, K. Folting, W.E. Streib, D.N. Hendrickson, G. Christou, Inorg. Chem. 35 (1996) 7578.
[17] J.B. Vincent, H.R. Chang, K. Folting, J.C. Huffman, G. Christou, D.N. Hendrickson, J. Am. Chem. Soc. 109 (1987) 5703.
[18] E.P. Serjeant, B. Dempsey, Ionisation Constants of Organic Acids in Aqueous Solution, Pergamon, New York, 1979.
[19] E. Libby, K. Folting, C.J. Huffman, J.C. Huffman, G. Christou, Inorg. Chem. 32 (1993) 2549.
[20] R.W. Taft, E.H. Cook, J. Am. Chem. Soc. 81 (1959) 46.
[21] E. Bouwman, K.G. Caulton, G. Christou, K. Folting, C. Gasser, D.N. Hendrickson, J.C. Huffman, E.B. Lobkovsky, J.D. Martin, P. Michel, H.-L. Tsai, Z. Xue, Inorg. Chem. 32 (1993) 3463.
[22] E. Libby, J.K. McCusker, E.A. Schmitt, K. Folting, D.N. Hendrickson, G. Christou, Inorg. Chem. 30 (1991) 3486.
[23] S. Wang, H.-L. Tsai, K. Folting, J.D. Martin, D.N. Hendrickson, G. Christou, J. Chem. Soc., Chem. Commun. (1994) 671.
[24] J.C. Jansen, H. Van Koningsveld, J.A.C. Van Ooijen, J. Reedijk, Inorg. Chem. 19 (1980) 170.
[25] S. Wang, PhD thesis, Indiana University, Bloomington, IN, 1993.
[26] T.J. Lane, A.J. Kandathil, S.M. Rosalie, Inorg. Chem. 3 (1964) 487.
[27] E.A. Schmitt, L. Noodleman, E.J. Baerends, D.N. Hendrickson, J. Am. Chem. Soc. 114 (1992) 6109.
[28] K. Kambe, J. Phys. Soc. Jpn 5 (1950) 48.
[29] J.H. Van Vleck, The Theory of Electric and Magnetic Susceptibilities, Oxford Press, London, 1932.